Thermo-mechanical behaviour of plain weave fabric composites: Experimental investigations

N. K. NAIK, V. K. GANESH
Aerospace Engineering Department, Indian Institute of Technology, Powai, Bombay – 400 076, India

An experimental investigation has been performed to elucidate the on-axes thermo-mechanical behaviour of two-dimensional orthogonal plain weave fabric laminates. Specifically T-300 carbon/epoxy and E-glass/epoxy systems were investigated for Young's modulus, inplane shear modulus, Poisson's ratio, linear thermal expansion coefficient, tensile strength and inplane shear strength. It is observed that there is a significant effect of weave geometrical parameters on the thermo-mechanical behaviour of woven fabric laminates. Properties of the woven fabric laminates are compared with the properties of the corresponding unidirectional balanced symmetric crossply laminates. A good correlation is observed between the experimental results and analytical predictions.

Nomenclature

List of symbols

a	strand width
C	crimp
$E_{fL}, E_{fT}, v_{fLT}, G_{fLT}, G_{fTT}$	elastic properties of the fibre along longitudinal and transverse directions
E_x, E_y, v_{xy}, G_{xy}	WF laminate elastic properties
g	gap between the adjacent strands
h	maximum strand thickness
h_m	thickness of pure matrix at $x = 0, y = 0$ in WF lamina
h_t	fabric thickness
H_L	total thickness of WF lamina
P	load
S	WF laminate inplane shear strength
S_f	fibre shear strength
t	laminate thickness
u	undulated length in interlacing region
V_f	fibre volume fraction
x, y, z	cartesian coordinates
X_{fT}	tensile failure strength of fibre along longitudinal direction
X_T	tensile failure strength
α_{fL}, α_{fT}	fibre co-efficient of thermal expansion along longitudinal and transverse directions
α_x	WF laminate linear thermal expansion coefficient
δ	displacement
ε_{fx}	fibre failure strain along longitudinal direction
ε_x	normal strain in x-direction
σ_x	normal stress in x-direction
ρ	density
ϕ	fibre diameter

SUPERSCRIPTS

o	overall properties
s	quantities of strand

SUBSCRIPTS

f	quantities in fill direction
w	quantities in warp direction

ABBREVIATIONS

CE1-CE4	Weave geometries: T-300 carbon/epoxy
CP	Balanced symmetric crossply laminate
C1,C2,C3	Configuration -1, -2, -3
Expt.	Experimental
FRP	Fibre reinforced plastic
GLE1-GLE8	Weave geometries: E-glass/epoxy
IOS	Iosipescu test
SD	Standard deviation
TEC	Linear thermal expansion coefficient
UD	Unidirectional
WF	Woven fabric
2D	Two-dimensional
10°	10° off-axis tension test
± 45°	± 45° off-axis tension test

0022–2461

1. Introduction

Increasing use is being made of woven fabric (WF) composites in high performance applications such as in the aerospace industry. In aerospace structural components, where optimal design concepts are employed, it is important to assess the extent to which each weave parameter has an effect on the thermo-mechanical behaviour of WF laminates.

Only a limited amount of experimental data on the thermo-mechanical behaviour of WF composites is currently available [1–7]. Dow and Ramnath [1] have studied the effect of weave pattern on the elastic and strength properties of WF laminates. Ishikawa *et al.* [2, 3] studied the effect of laminate thickness on the elastic properties and the nonlinear stress–strain behaviour of WF laminates. In addition some experimental data on the thermo-elastic behaviour of WF laminates are presented in references [4–7]. Experimental investigations on the thermal behaviour of thick glass/epoxy composites have been presented by Raghava *et al.* [8] and results of a linear thermal expansion coefficient (TEC) study on WF laminates are presented in reference [9]. For all the earlier works, the experimental investigation specifically served to validate the analytical methods. Therefore a complete and exhaustive experimental survey to determine the effect of weave geometry on the thermo-mechanical behaviour of WF laminates is currently unavailable. In the present work, the effect of weave geometry on all aspects of the thermo-mechanical behaviour of two-dimensional (2D) orthogonal plain weave fabric laminates has been investigated. For some properties, more than one method has been used to study the suitability of the particular method for WF composites. In the present paper, two different material systems with twelve weave geometries have been considered in the study of the on-axes thermo-mechanical behaviour of 2D orthogonal plain weave fabric laminates.

2. Experimental techniques

2.1. Young's modulus, Poisson's ratio and tensile strength

Tests were conducted to determine the Young's modulus, the Poisson's ratio and normal tensile strength according to the procedures of ASTM test D3039. The tensile specimens were 25 mm wide with a nominal thickness of 2 mm. The specimens were tested on a Lloyd M50K machine at room temperature (27 °C) at a crosshead speed of 1 mm per min.

The strain was measured using an electrical resistance strain gauge and a 25 mm gauge length extensometer. The gauge length of the strain gauge was such that the gauge is spread over a few interlacings so as to measure the average strain. In the present study foil gauges with a 6 mm gauge length and a 120 Ω resistance supplied by Tokyo Sokki Kenkyujo Co., Ltd. were used.

An extensometer was used to measure the strain at higher stress at which point the matrix between the strands begins to give way. At this stress, the strains in the failed region are high and may exceed the strain limit of the normal foil gauges, and the failure initiation may not be at the section at which the strain gauge is fixed. By using an extensometer of gauge length 25 mm, there is a greater probability of capturing these strains and in addition the extensometer could measure strains upto 20%. It should be noted that specimen tapering to induce a failure at a specific section is not recommended for fibre reinforced composites.

2.2. Inplane shear modulus and strength

The ideal quantitative shear test method should provide a region of pure, uniform shear stress. In addition, there should be a unique relationship between the applied load and the magnitude of the shear stress in the test section. Further, for accurate determination of the shear stress–shear strain response, the test section should be one of maximum shear stress relative to all other regions of the specimen.

Lee and Munro [10] have examined and discussed the merits and disadvantages of different inplane shear test methods with respect to unidirectional (UD) composites. They used a decision analysis technique for the evaluation of inplane shear test methods with the cost of fabrication, cost of testing, data producibility and accuracy of experimental results as criteria. Although the thin-walled tube torsion test was rated on top in terms of the quality of the data produced, it was ranked low overall because of the high cost of specimen fabrication and testing. Overall, they have rated $\pm 45^\circ$ off-axis tension test, the Iosipescu test and the 10° off-axis tension test as the best methods. These methods are frequently used in the literature for the determination of inplane shear modulus and strength of fibre reinforced plastic (FRP) composites [11–19].

In UD composites, a low off-axis angle, i.e., 10° off-axis tension test was used to estimate the nonlinear shear response and the strength as the transverse stress does not affect the failure significantly at low off-axis angles. The 10° off-axis tension test is not recommended for the evaluation of the initial shear response because of end-constraint shear coupling effects. The $\pm 45^\circ$ off-axis tension test is an excellent test method for the determination of shear modulus, but is not a good test method for the characterization of the nonlinear response and determination of shear strength because the specimen fails at a low level of strain due to transverse stresses. An attractive alternate to the off-axis tension test for the determination of both the initial shear modulus and ultimate shear strength is the Iosipescu test.

In the present study, the inplane shear modulus was determined from 10° and $\pm 45^\circ$ off-axis tension tests while the inplane shear strength was determined using the Iosipescu test in addition to 10° and $\pm 45^\circ$ off-axis tension tests. The specimen geometry and test conditions for the tension test were as per ASTM test D 3039. The specimens were instrumented with electrical resistance gauge rosettes to measure the longitudinal, transverse and the strain at 45° to the specimen

axis. The Iosipescu specimen for the evaluation of inplane shear strength was prepared as per reference [18].

2.3. Linear thermal expansion coefficient (TEC)

The thermal induced strains are usually measured with the help of strain gauges or a dilatometer. The change in resistance of the strain gauge grid is measured which in turn reflects the strain in the material. The dilatometer physically measures the deformation of the specimen due to the change in temperature from which the laminate TEC can be calculated. Both these methods have certain limitations when used to measure the TEC of WF laminates. In the strain gauge method the correct temperature compensation to be applied is the limitation while a possible non-uniform temperature distribution along the length of the specimen forms the limitation in the dilatometer technique. The compensation for the change in the performance in the gauge characteristics due to the change in temperature can be either done using the apparent strain–temperature and gauge factor–temperature curves or by using a reference gauge mounted on a substrate of known TEC. The gauge characteristic curves are valid only for the material on which the test was conducted to produce these curves and for materials with a matching TEC. In cases where a reference gauge is used for temperature compensation, care should be taken to see that the reference gauge is mounted on a substrate which has a TEC vastly different from that of the material under test. In the present work, both the methods, i.e., the strain gauge method and the dilatometer method have been used to determine the TEC of the plain weave fabric laminates.

3. Experimental details

A comprehensive experimental programme was planned to generate a data bank on the on-axes thermo-mechanical properties of orthogonal plain weave fabric composites. The effect of the weave geometry on the thermo-mechanical behaviour of plain weave fabric laminates was studied using these results.

The experiments were carried out on four different types of carbon/epoxy and eight different types of E-glass/epoxy laminates. The epoxy resin LY556 with hardener HY951 supplied by Cibatul, India was used. The thermo-elastic properties of T-300 carbon and E-glass fibres and the resin are presented in Table I [20]. The strength properties are presented in Table II. The strengths of the fibres were calculated from experimentally measured UD lamina strength [21]. The epoxy resin properties are for the bulk material.

The four types of carbon fabrics/laminates/material systems are designated as CE1, CE2, CE3 and CE4 whereas the eight types of E-glass fabrics/laminates/material systems are designated as GLE1–GLE8. The corresponding strand and fabric properties are presented in Tables III and IV. Typical maximum undulation angles for fill strand are as follows: for GLE1 it is 5.9° whereas for GLE6 it is 11.4°. It may be noted that only GLE1 and GLE2 are balanced fabrics. For a balanced plain weave fabric, not only are the number of counts and crimp the same along both the warp and fill directions but also the strand width (a), strand thickness (h) and inter-strand gap (g) are the same along both directions. In addition to this, the strand properties are the same along both the warp and fill directions. For GLE7, the strand was slightly twisted. The laminates were prepared at room temperature in a specially designed matched die mould. The laminate details are given in Table V. The geometrical parameters of the fabric were determined by means of an

TABLE I Thermo-elastic properties of fibres and matrix

Material	E_{fL} (GPa)	E_{fT} (GPa)	G_{fLT} (GPa)	G_{fTT} (GPa)	ν_{fLT}	α_{fL} (ppm per °C)	α_{fT} (ppm per °C)	ρ (gm cc^{-1})
Fibre								
T-300 Carbon	230.0	40.0	24.0	14.3	0.26	− 0.7	10.0	1.76
E-Glass[a]	72.0	72.0	27.7	27.7	0.30	5.4	5.4	2.62
Matrix								
Epoxy resin[a]	3.5	3.5	1.3	1.3	0.35	63.0	63.0	1.17

(a) Isotropic

TABLE II Strength properties of fibres and matrix

Material	Longitudinal tensile strength, X_{fT} (MPa)	Shear strength, S_f (MPa)	Failure strain, ε_{fx} (%)	Fibre diameter, ϕ (μm)
T-300 Carbon	2475.0[b]	–	1.3	7
E-Glass[a]	1995.0[b]	–	4.8	10–20
Epoxy Resin[a]	60.0	100.0	3.0	–

[a] Isotropic
[b] Practical value – calculated from UD lamina properties

TABLE III Strand and fabric properties

Material	Fabric thickness, h_t (mm)	Fabric weight ($gm\,m^{-2}$)	Crimp, C (%)		No. of counts (per cm)		Strand tex ($gm\,km^{-1}$)	
			Fill	Warp	Fill	Warp	Fill	Warp
T-300 Carbon								
CE1	0.200	160	0.15	0.15	4	4	200	170
CE2	0.200	160	0.15	0.15	4	4	170	200
CE3	0.160	130	0.30	0.30	8.8	8.8	61	68
CE4	0.160	130	0.30	0.30	8.8	8.8	68	61
E-Glass								
GLE1	0.085	75	0.26	0.26	15	15	22	22
GLE2	0.095	100	0.25	0.25	14	14	30	30
GLE3	0.180	210	0.96	0.96	14	14	75	71
GLE4	0.180	210	0.96	0.96	14	14	71	75
GLE5	0.220	300	0.99	0.99	12	12	150	140
GLE6	0.220	300	0.99	0.99	12	12	140	150
GLE7	0.450	525	1.62	1.62	7	7	370	370
GLE8	0.180	209	0.84	1.37	13	17	70	70

TABLE IV Plain weave fabric structure $u/a = 1.0$, $h_w = h_f = h_t/2$

Material	Fabric thickness, h_t (mm)	Fill strand			Warp strand		
		a_f (mm)	h_f (mm)	g_f (mm)	a_w (mm)	h_w (mm)	g_w (mm)
T-300 Carbon							
CE1	0.200	1.80	0.100	0.65	1.45	0.100	1.00
CE2	0.200	1.45	0.100	1.00	1.80	0.100	0.65
CE3	0.160	0.96	0.080	0.18	1.10	0.080	0.04
CE4	0.160	1.10	0.080	0.04	0.96	0.080	0.18
E-Glass							
GLE1	0.085	0.40	0.043	0.25	0.40	0.043	0.25
GLE2	0.095	0.45	0.048	0.30	0.45	0.048	0.30
GLE3	0.180	0.68	0.090	0.04	0.62	0.090	0.10
GLE4	0.180	0.62	0.090	0.10	0.68	0.090	0.04
GLE5	0.220	0.86	0.110	0.00	0.84	0.110	0.02
GLE6	0.220	0.84	0.110	0.02	0.86	0.110	0.00
GLE7	0.450	1.08	0.225	0.30	1.21	0.225	0.17
GLE8	0.180	0.60	0.090	0.17	0.60	0.090	0.00

TABLE V Properties of WF laminae/laminates

Material	Fabric thickness, h_t (mm)	Laminate – no. of layers	Laminate thickness, t (mm)	V_f^0	Lamina thickness, H_L (mm)
T-300 Carbon/epoxy					
CE1	0.20	10	1.90	0.39	0.200
CE2	0.20	10	1.90	0.39	0.200
CE3	0.16	12	1.95	0.44	0.162
CE4	0.16	12	1.95	0.44	0.162
E-Glass/epoxy					
GLE1	0.085	18	1.55	0.28	0.086
GLE2	0.095	15	1.50	0.23	0.100
GLE3	0.180	10	1.80	0.40	0.180
GLE4	0.180	10	1.80	0.43	0.180
GLE5	0.220	7	1.55	0.46	0.221
GLE6	0.220	7	1.55	0.47	0.221
GLE7	0.450	6	2.70	0.41	0.450
GLE8	0.180	8	1.52	0.38	0.190

optical microscope at a magnification of $\times 20$ and using photomicrographs of the laminate cross-sections.

Static tensile test specimens were cut from a laminate of size 300 mm $\times$ 300 mm and machined to the geometry as specified by ASTM specification D 3039.

Iosipescu shear tests were performed using a modified Iosipescu test fixture and the specimen geometry developed by Walrath and Adams [18]. The specimens were tested at room temperature (27 °C) under a controlled displacement of 1 mm per min. The fill direction was along the length of the specimen.

For the determination of the TEC, specimens of length 100 mm and width 20 mm were used. The specimens were dried in an oven at a temperature of 50 °C for 24 h to remove any moisture, present in the specimen. For specimens with strain gauges the test temperature was varied from (− 30°)C to room temperature (27°)C. The strain readings were taken at an interval of 10 °C. The apparent strain and gauge factor corrections applied were based on the gauge characteristic curves for a gauge mounted on mild steel. Although this procedure is not recommended for composites, precautions were taken so as to minimize the error due to this procedure. The selected test temperature was such that it falls on either side of the zero apparent strain thereby reducing the effect of correction on the final results. Also the TEC of the glass/epoxy material system in the symmetric crossply configuration and the fibre volume fraction (V_f) used in the present study is not significantly different from that of mild steel.

In the case of the TEC determined using a dilatometer, the test was conducted in a temperature range from room temperature (27°)C to (50°)C. The other test specifications are as per ASTM test specification D 696.

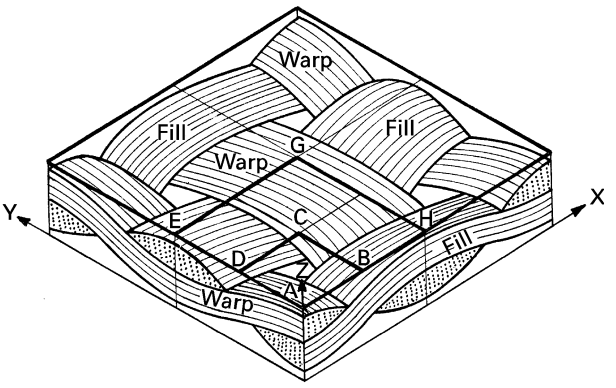

Figure 1 Idealized representative plain weave fabric lamina.

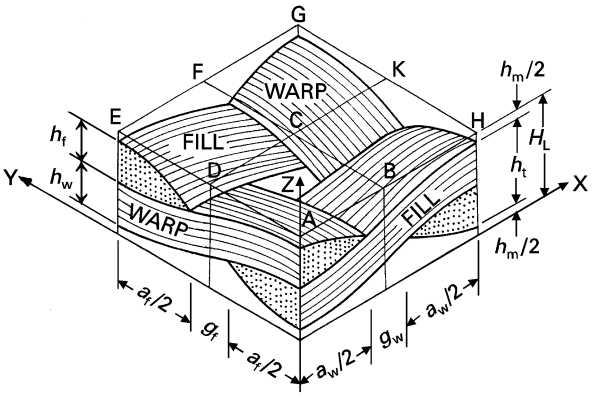

Figure 2 Plain weave fabric lamina geometrical representative unit cell.

4. Analytical predictions

Two-dimensional analytical models have been used for the prediction of the thermo-mechanical behaviour of woven fabric laminates [4–7, 22–25]. These methods consider strand undulation and continuity along both the warp and fill directions, the actual cross-sectional geometry of the strand and the fabric geometry and the actual laminate configuration including the possible shifts of layers with respect to each other during lamination.

An idealized representative plain weave fabric lamina is shown in Fig. 1. A geometrical representative unit cell showing all the weave parameters considered in the 2D analytical models is shown in Fig. 2. This consists of resin imperganated warp and fill strands and pure matrix regions. The 2D WF composite stiffness model is used for predicting the thermo-elastic behaviour [4–7]. The 2D WF composite strength model takes into account the material and geometrical nonlinearities and predicts the complete stress-strain history upto ultimate failure [22–25]. Different stages of failure such as warp strand transverse failure, fill strand shear/transverse failure, pure matrix block failure and the failure of matrix and fibre in the fill strand under longitudinal tension are predicted. For the prediction of the thermo-mechanical properties, the actual laminate is idealized into three configurations as is shown in Fig. 3. In configuration-1 (C1), there is no relative shift between the adjacent layers. In configuration-2 (C2), the adjacent layers are shifted with respect to each other by a distance $(a + g)/2$ both in the fill and warp directions. By

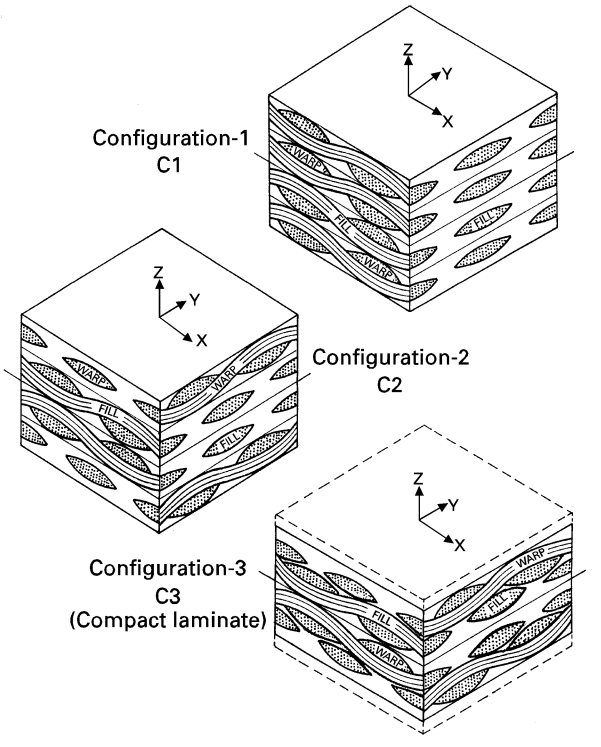

Figure 3 Stacking of layers in different idealized laminate configurations.

giving a maximum possible shift to the layers in the laminate C2 in the thickness direction (z-direction) such that the peaks of one layer enter into the valleys of the adjacent layers, the laminate configuration-3

(C3) is formed. The laminates in configuration-3 are termed as compact laminates.

5. Results and discussion

The fibre and matrix properties, fabric weave geometrical parameters and the laminate details are presented in Tables I–V. The experimentally determined and analytically predicted on-axes thermo-mechanical properties of the plain weave fabric laminates are presented in Tables VI–XI. The experimental results, in general, are the averages of five test data. The property translation efficiency factor equal to unity was used to derive the properties of the strand from those of a single filament for analytical predictions.

TABLE VI Experimental and predicted Young's moduli of plain weave fabric laminates (GPa)

Material system		Experimental, E_x		Predicted, E_x				
	V_f^0 C1, C2	E_x	SD	C1	C2	C3	UD at V_f^0	CP at V_f^0
CE1	0.27	62.5	3.2	42.0	42.6	63.4	64.7	35.6
CE2	0.27	–	–	32.2	32.7	48.6	64.7	35.6
CE3	0.44	49.3	1.9	49.8	50.2	67.7	103.1	56.0
CE4	0.44	60.3	2.1	56.7	57.6	77.6	103.1	56.0
GLE1	0.28	17.5	1.0	13.5	14.0	21.3	22.6	14.6
GLE2	0.23	20.0	0.8	14.0	14.6	22.2	19.2	12.6
GLE3	0.40	21.5	1.0	19.2	19.8	26.5	30.9	19.7
GLE4	0.43	20.8	0.7	21.2	21.9	28.8	32.9	21.0
GLE5	0.46	22.8	1.2	21.3	21.8	28.5	35.0	22.4
GLE6	0.47	22.4	1.0	21.7	22.2	29.0	35.7	22.9
GLE7	0.41	19.6	1.3	18.7	19.6	27.4	31.6	20.2
GLE8	0.38	–	–	17.3	18.2	25.0	29.5	18.8

TABLE VII Experimental and predicted inplane shear moduli of plain weave fabric laminates (GPa)

Material system		Experimental, G_{xy}			Predicted, G_{xy}				
	V_f^0 C1, C2	10°	± 45°	IOS	C1	C2	C3	UD at V_f^0	CP at V_f^0
CE1	0.27	10.00	5.00	–	3.19	3.43	5.11	2.10	2.10
CE2	0.27	–	–	–	2.83	3.05	4.54	2.10	2.10
CE3	0.44	–	–	–	4.65	4.75	6.40	2.90	2.90
CE4	0.44	–	–	–	4.59	4.87	6.56	2.90	2.90
GLE1	0.28	–	–	–	2.71	2.92	4.41	2.15	2.15
GLE2	0.23	6.25	2.94	–	2.88	3.14	4.75	1.96	1.96
GLE3	0.40	6.89	3.57	–	3.74	3.92	5.28	2.70	2.70
GLE4	0.43	–	–	–	4.39	4.59	6.05	2.90	2.90
GLE5	0.46	8.33	5.50	–	4.32	4.49	5.85	3.10	3.10
GLE6	0.47	–	–	–	4.46	4.62	6.02	3.20	3.20
GLE7	0.41	–	–	–	4.20	4.46	6.23	2.80	2.80
GLE8	0.38	7.14	3.84	–	3.72	3.85	5.28	2.60	2.60

TABLE VIII Experimental and predicted Poisson's ratios of plain weave fabric laminates

Material system		Experimental, ν_{xy}	Predicted, ν_{xy}				
	V_f^0 C1, C2	ν_{xy}	C1	C2	C3	UD at V_f^0	CP at V_f^0
CE1	0.27	0.10	0.166	0.076	0.076	0.321	0.056
CE2	0.27	–	0.131	0.059	0.059	0.321	0.056
CE3	0.44	–	0.080	0.059	0.059	0.306	0.046
CE4	0.44	–	0.110	0.066	0.066	0.306	0.046
GEL1	0.28	–	0.238	0.192	0.192	0.333	0.145
GEL2	0.23	–	0.243	0.198	0.198	0.336	0.153
GEL3	0.40	–	0.209	0.187	0.187	0.327	0.137
GEL4	0.43	–	0.197	0.181	0.181	0.325	0.137
GEL5	0.46	–	0.202	0.188	0.188	0.324	0.137
GEL6	0.47	–	0.203	0.189	0.189	0.323	0.136
GEL7	0.41	–	0.208	0.188	0.188	0.326	0.136
GEL8	0.38	–	0.177	0.166	0.166	0.328	0.137

TABLE IX Experimental and predicted linear thermal expansion coefficients of plain weave fabric laminates (ppm per °C)

Material system	V_f^0 C1, C2	Experimental, α_x		Predicted, α_x				
		SG	DM	C1	C2	C3	UD at V_f^0	CP at V_f^0
CE1	0.27	5.31	5.68	5.11	5.79	5.79	1.91	8.26
CE2	0.27	6.04	8.33	7.75	8.44	8.44	1.91	8.26
CE3	0.44	–	–	4.89	5.38	5.38	0.56	4.98
CE4	0.44	–	–	3.92	4.16	4.16	0.56	4.98
GLE1	0.28	20.86	21.12	19.88	20.47	20.47	11.88	22.90
GLE2	0.23	19.58	19.51	19.29	19.78	19.78	13.53	25.53
GLE3	0.40	13.69	15.45	15.58	15.73	15.73	9.40	18.39
GLE4	0.43	–	–	14.82	14.83	14.83	8.97	17.55
GLE5	0.46	12.88	14.06	14.76	14.80	14.80	8.59	16.73
GLE6	0.47	–	–	14.29	14.31	14.31	8.47	16.46
GLE7	0.41	15.20	18.60	15.88	15.77	15.77	9.25	18.10
GLE8	0.38	–	–	17.80	17.71	17.71	9.72	18.97

TABLE X Experimental and predicted ultimate tensile failure strengths of plain weave fabric laminates (MPa)

Material system	V_f^0 C1, C2	Experimental, X_T		Predicted, X_T				
		X_T	SD	C1	C2	C3	UD at V_f^0	CP at V_f^0
CE1	0.27	573	31.2	493	510	586	680	340
CE2	0.27	504	16.2	370	330	511	680	340
CE3	0.44	490	13.2	474	490	636	1110	557
GLE1	0.28	244	15.1	218	248	320	611	307
GLE2	0.23	262	21.0	215	245	316	512	256
GLE3	0.40	318	5.9	304	346	362	856	430
GLE4	0.43	320	6.2	320	363	382	914	458
GLE5	0.46	367	8.0	321	364	373	970	487
GLE6	0.47	338	10.1	322	365	381	989	497
GLE7	0.41	252	10.2	308	353	370	875	440
GLE8	0.38	–	–	282	327	345	818	411

TABLE XI Experimental and predicted inplane shear strengths of plain weave fabric laminates (MPa)

Material system	V_f^0 C1, C2	Experimental, S			Predicted, S				
		10°	± 45°	IOS	C1	C2	C3	UD at V_f^0	CP at V_f^0
CE1	0.27	51	42	65	81	67	62	98.2	98.2
CE2	0.27	–	–	–	91	64	64	98.2	98.2
CE3	0.44	–	–	–	78	70	72	101.3	101.3
GLE1	0.28	–	–	–	35	25	24	36.0	36.0
GLE2	0.23	28	26	33	32	26	24	35.9	35.9
GLE3	0.40	27	24	34	34	27	28	36.6	36.6
GLE4	0.43	–	–	–	34	28	28	36.8	36.8
GLE5	0.46	30	26	39	34	28	29	37.1	37.1
GLE6	0.47	–	–	–	34	28	29	37.2	37.2
GLE7	0.41	–	–	–	34	27	27	36.7	36.7
GLE8	0.38	28	26	37	34	27	27	36.5	36.5

From Table V, it is seen that the fabric thickness multiplied by the number of layers in the laminate is nearly equal to the laminate thickness for all the WF laminates except for CE1 and CE2. This indicates that the pure matrix layer is not present between two fabric layers. In the cases of CE1 and CE2, the actual laminate thickness is less than the fabric thickness multiplied by the number of layers. This indicates the possibility of some z-shift in these laminates. The possible reasons for this could be the larger gap between adjacent strands in both the fill and warp directions and a lower inter-fibre friction of carbon fibres compared to glass fibres.

In general, in an actual laminate, compaction may not take place due to constraints on the relative lateral movement of layers during lamination, friction

between fabric layers, local departure in strand perpendicularity and the possible variation of number of counts from place to place in a fabric. Therefore an actual laminate would have scattered zones of C1, C2 and C3. From the photomicrographic studies, it can be reasonably inferred that the C2 laminate configuration occurrence is the most probable. This observation has also been made by Jortner [26]. Now, from Tables VI–XI, comparing the experimental and predicted results it is clear that most of the experimental results closely match those of C2 predictions except for CE1 and CE2.

The experimentally determined overall fibre volume fraction (V_f^0) for all the material systems considered are presented in Table V. It is seen that, the fabrics with a smaller gap have a higher V_f^0 while fabrics with a larger gap have a lesser V_f^0. In the case of CE1 and CE2, the laminates have a higher V_f^0 even though these fabrics have larger gaps between adjacent strands due to a certain amount of compaction having taken place in these laminates.

Table VI presents the experimental and predicted Young's moduli. It is observed that the Young's modulus is smaller for laminates with smaller V_f^0 and higher for laminates with fabrics having lesser crimp. In the case of CE1, although the V_f^0 is smaller than for CE3, the crimp of CE1 being substantially smaller than for CE3, the Young's modulus is higher for CE1. This is true to a certain extent for GLE1 and GLE2. In the case of GLE3, GLE4, GLE5 and GLE6, although the crimp is higher for GLE5 and GLE6, the Young's modulus is also higher than for GLE3 and GLE4 since V_f^0 is higher. Comparing the Young's modulus of WF laminates with that of the Young's modulus of UD balanced symmetric crossply laminate (CP) at V_f^0 it is seen that all the laminates made of fabric with smaller gaps have a Young's modulus marginally smaller than the corresponding CP. For laminates with fabrics having a larger gap, the Young's modulus of CP is smaller than that of the Young's modulus of the corresponding WF laminates. This is because the effect of the gap in reducing the V_f^0 of WF laminate is significant. The reduction in V_f^0 reduces the Young's modulus of CP significantly whereas the reduction in the Young's modulus of WF laminate is not significant. As expected, the Young's modulus of a UD laminate at V_f^0 is always greater than that of the Young's modulus of the corresponding WF laminate.

The shear modulus determined using the 10° and $\pm 45^\circ$ off-axis tension tests and the predicted shear modulus values are presented in Table VII. As expected, due to the reasons mentioned previously, the shear modulus values obtained from the 10° off-axis test are significantly higher than those obtained from the $\pm 45^\circ$ off-axis test and the predicted values. The $\pm 45^\circ$ off-axis test results compare closely with the predicted shear modulus values. It can be distinctly observed that the shear modulus increases with an increase in crimp. Comparing the WF laminate shear modulus with those of UD and CP at V_f^0, it is seen that WF laminate shear modulus values are appreciably higher. This could be due to the interlacing of strands in WF composites.

The Poisson's ratio values are presented in Table VIII. The WF laminate Poisson's ratio values are higher than those of the corresponding CP at V_f^0. This is because of the undulations present in the case of WF laminates. The Poisson's ratio values for the UD laminate are significantly higher than those of the corresponding WF laminate values. This is because there is a constraint to transverse deformation from the warp strand in WF laminates, whereas, this is not present in UD laminates.

The TEC determined using the strain gauge and dilatometer techniques are presented in Table IX. The predicted TEC values for the WF, UD and CP laminates are also presented. It is seen that the TEC values for all the material systems measured using the dilatometer compare closely with the predicted values. The TEC determined using the strain gauge technique closely matches the predicted values for CE1, GLE1 and GLE2 whereas for the other material systems there is some error. From the dilatometer results it is seen that laminates with a lower V_f^0 have a higher TEC. In the case of CE1 and CE2, although V_f^0 is the same for both laminates, the TEC is higher for CE2 because of the smaller fill strand width. Although the V_f^0 is almost same for GLE3 and GLE7, the TEC is higher for GLE7 due to the larger crimp for GLE7. The TEC of the UD laminate at V_f^0 is significantly lower than that of the WF laminate, whereas, the WF laminates TEC is marginally smaller than that of the CP laminate at V_f^0.

The experimental and predicted ultimate tensile failure strengths for the considered material systems are listed in Table X. For comparison, the predicted UD and CP strengths at V_f^0, are also presented. By comparing the experimental and predicted strength values it is seen that most of the experimental results fall in-between the C1 and C2 predictions except for CE1, CE2 and GLE7. In the cases of CE1 and CE2, the experimental values are nearer to the C3 prediction while for GLE7 the experimental results are

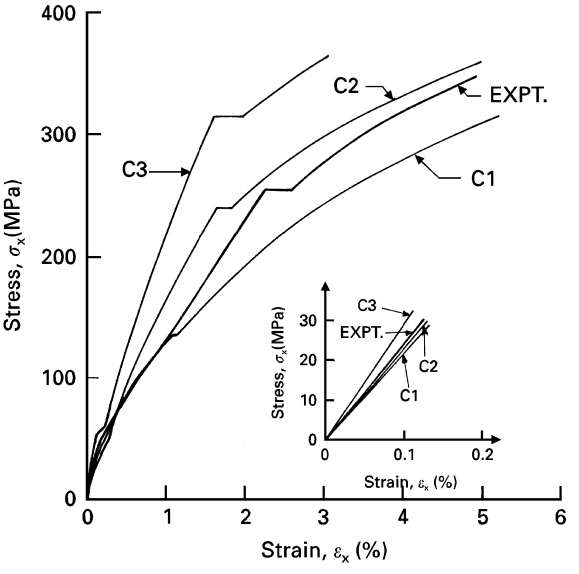

Figure 4 Predicted and experimental stress–strain behaviour for E-glass/epoxy laminate GLE5. The values of $V_f^0 = 0.46$ (Expt) and $V_f^s = 0.74$ should be noted.

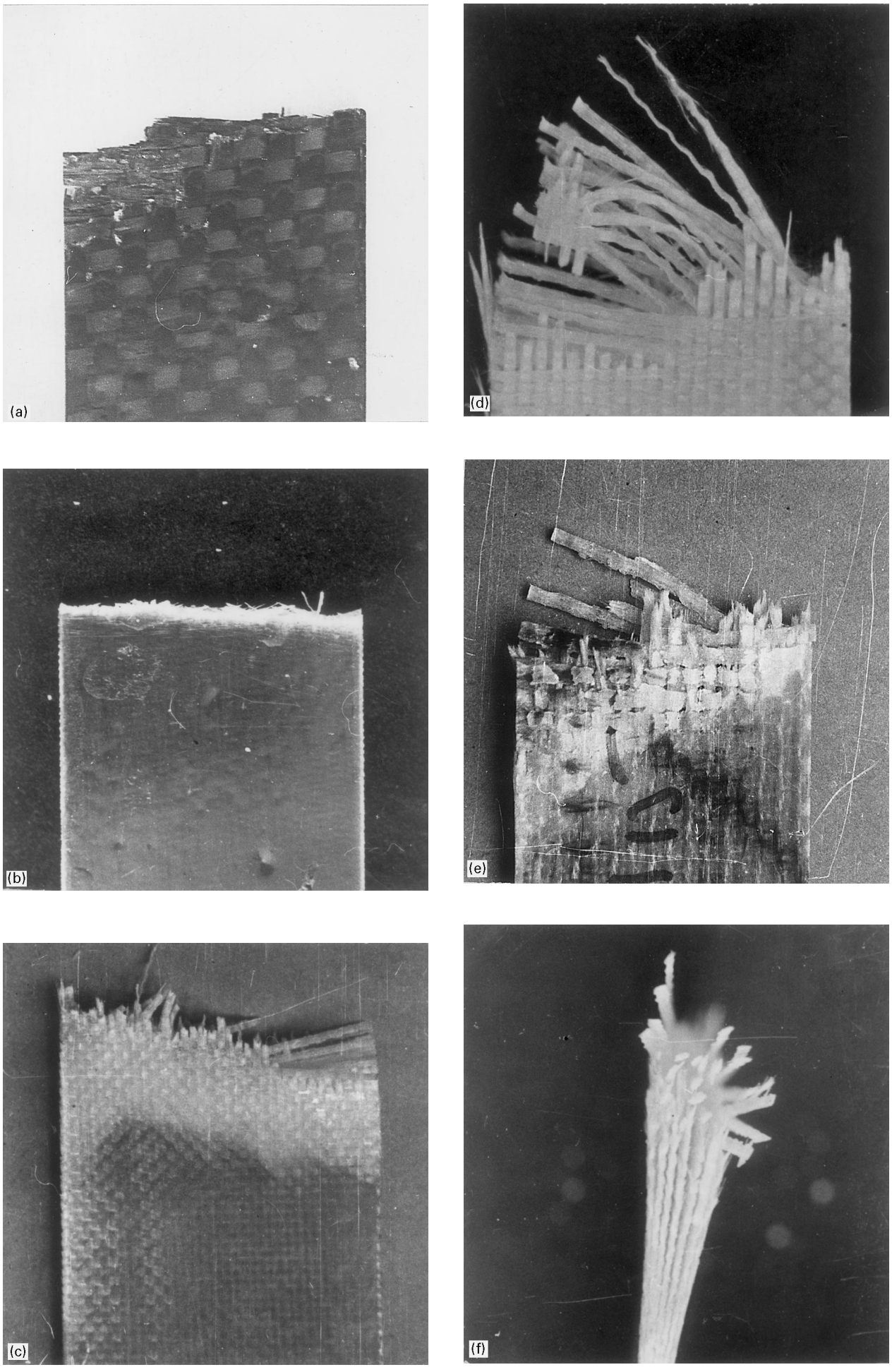

Figure 5 Failure modes of typical plain weave fabric specimens.

smaller than even the C1 prediction. For CE1 and CE2, as indicated earlier, there is some compaction and hence it is logical for the results to be higher than the C2 prediction. In the fabric GLE7 the strands were slightly twisted and therefore a reduction in the experimental strength is observed. The predictions are based on straight strands since a fibre to strand translation efficiency factor of unity was taken. It is interesting to note that the twist in the strand increases the Young's modulus whereas it reduces the ultimate failure strength in the case of the E-glass/epoxy material system (GLE7). This could be because the glass fibres are isotropic and therefore the reduction in stiffness due to twist is not significant. The twisting of strands can suppress the effect of local defects in the strand during initial loading and hence there is the possibility of increased stiffness. However, the twist can introduce a considerable amount of bending stress which in turn causes early failure. Here also, as in the case of the Young's modulus, a higher V_f^0 gives a higher failure strength while a higher crimp produces a lower failure strength.

The experimental and predicted stress–strain plots under normal loading upto the ultimate failure for GLE5 are shown in Fig. 4. The plots show a nonlinear stress-strain behaviour. There are two distinct points on the stress-strain curve where the slope of the curve changes steeply. The first one is at a stress of 50 MPa and is due to the warp strand transverse failure while the second is at about 250 MPa and is due to the failure of the matrix in the pure matrix pocket. The strains used to plot the experimental stress–strain curve were measured using a 25 mm gauge length extensometer. Fig. 5 shows the micrographs of the failed edge of the specimen. It is seen that the area of failure is different for different material systems and that it is not uniform over the gauge length of the extensometer. The representative strain of the specimen would be the average strain within a failed unit cell and hence the strain sensed by the extensometer will have to be corrected. The total deformation within the gauge length of the extensometer is the sum of the elastic deformation of the unfailed region and the total deformation in the localized damage region. The total deformation within the gauge length of the damaged region was noted and then the elastic deformation of the undamaged length within the gauge length was calculated. From the total deformation and the deformation of the undamaged part of the specimen within the gauge length, the deformation within the damaged length was calculated. From this the deformation in an individual unit cell and the corresponding strain were calculated.

The load–displacement curves for 10° off-axis and $\pm 45°$ off-axis tension tests are presented in Fig. 6. The predicted and experimental shear stress–shear strain behaviour for E-glass/epoxy laminate GLE2 is presented in Fig. 7. The deformation for a 10° test is considerably smaller than that for the $\pm 45°$ test at ultimate failure. In the case of the $\pm 45°$ test, the bulk of the deformation takes place after the shear failure. This can be attributed to the reorientation of the strands after the failure of the pure matrix pockets.

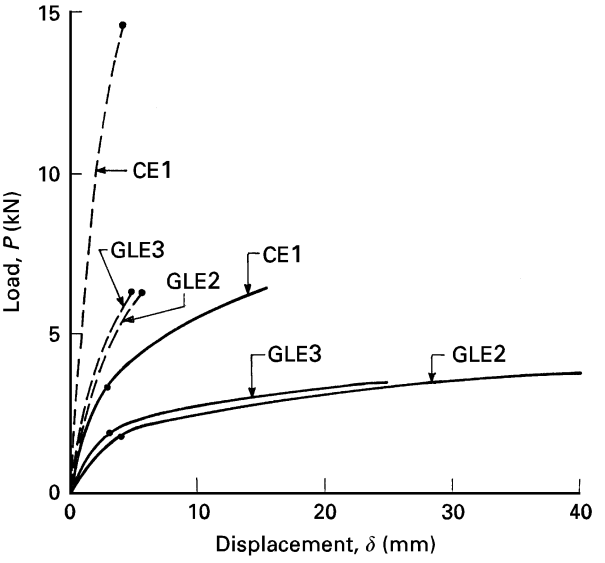

Figure 6 Load–displacement curves for (– – –) 10° and (——) $\pm 45°$ off-axis tension tests for a plain weave fabric laminate.

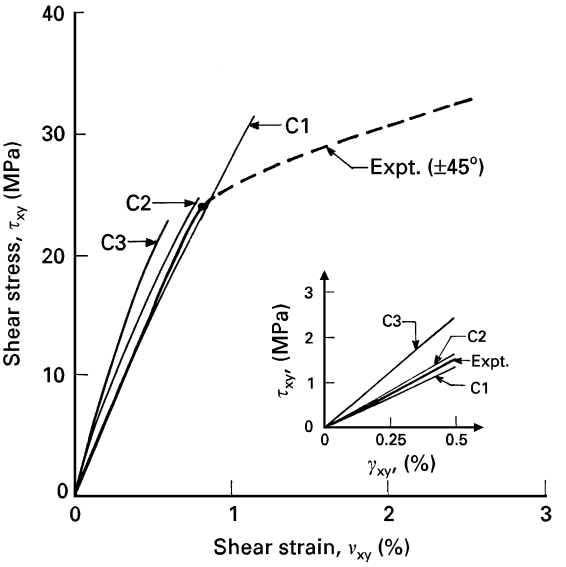

Figure 7 Predicted and experimental shear stress–shear strain behaviour for E-glass/epoxy laminate GLE2. The values of $V_f^0 = 0.23$ (Expt) and $V_f^s = 0.74$ should be noted.

A sudden increase in deformation, i.e., a sudden change in the slope of the load–displacement curve indicates the shear failure. The load at this corresponding point is taken as the load at which the shear failure has taken place. These points are indicated as solid circles on the load–displacement curves (Fig. 6). We note that for the 10° off-axis test, the shear failure load and the ultimate load are the same. The inplane shear strengths, presented in Table XI, are calculated based on the load as indicated by the solid circles on the load–displacement curves. A similar procedure was adopted for the determination of the inplane shear strength using the Iosipescu test.

As can be seen from Table XI, the experimental inplane shear strengths obtained by the 10° and $\pm 45°$ off-axis tension tests are nearly equivalent. The Iosipescu test gives a higher inplane shear strength.

In the case of WF laminates, the $\pm 45^\circ$ off-axis test specimens give a better shear response because of the interlacing of strands. We note that, for the $\pm 45^\circ$ off-axis test specimens, a fibre pull out mode of failure takes place in UD composites, whereas, the ultimate failure of WF composites is by fibre breakage. The possible drawbacks in the $\pm 45^\circ$ off-axis test for UD composite are eliminated in the case of WF composites. Hence, the $\pm 45^\circ$ off-axis tension test is also suitable for inplane shear strength evaluation for WF composites. As in the case of the UD composites, the $\pm 45^\circ$ off-axis tension test is also suitable for determination of the inplane shear modulus for WF composites. Hence, the $\pm 45^\circ$ off-axis tension test can be used to characterize the initial as well as the ultimate shear response of WF laminates.

Comparing the shear strength of GLE2, GLE3, GLE5 and GLE8 it is observed that there is no significant effect of the weave geometry of V_f^0 on the inplane shear strength of WF laminates. Although the T-300 carbon/epoxy and E-glass/epoxy have the same matrix, the T-300 carbon/epoxy laminates show a higher shear strength. Comparing the inplane shear strength of WF, UD and CP laminates at V_f^0 it is seen that UD and CP laminates have a higher shear strength. This could be due to shear stress concentration in the strands in WF laminates.

6. Conclusions

A comprehensive experimental programme was performed in order to investigate the thermo-mechanical behaviour of 2D orthogonal plain weave fabric laminates. The experimental results were compared with analytical predictions. It is seen that as the gap increases, V_f^0 decreases. With an increase in V_f^0 and a decrease in crimp, an increase in the Young's modulus and tensile failure strength is observed. There is no significant effect of crimp on the inplane shear modulus and strength. A higher V_f^0 gives a lower TEC. Overall, it is observed that the weave geometrical parameters have a significant effect on the thermo-mechanical behaviour of WF laminates. A close correlation between the experimental results and the analytical predictions is observed.

Acknowledgements

This work was supported by the Structures Panel, Aeronautics Research & Development Board, Ministry of Defence, Government of India, Grant No. Aero/RD-134/100/10/90–91/659.

References

1. N. F. DOW and V. RAMNATH, Analysis of woven fabrics for reinforced composite materials, NASA-CR-178275 (1987).
2. T. ISHIKAWA, M. MATSUSHIMA, Y. HAYASHI and T. W. CHOU, *J. Compos. Mater.* **19** (1985) 443.
3. T. ISHIKAWA, M. MATSUSHIMA and Y. HAYASHI, *AIAA Journal* **25** (1987) 107.
4. N. K. NAIK and P. S. SHEMBEKAR, *J. Compos. Mater.* **26** (1992) 2196.
5. P. S. SHEMBEKAR and N. K. NAIK, *ibid.* **26** (1992) 2226.
6. N. K. NAIK and V. K. GANESH, *Compos. Struct.* **26** (1993) 139.
7. V. K. GANESH and N. K. NAIK, *Compos. Sci. Tech.* **51** (1994) 387.
8. R. S. RAGHAVA, J. VALENTICH and R. D. NATHENSON, *J. Compos. Mater.* **18** (1984) 81.
9. P. CIRESE and A. CORVI, in Composite Structures 5 edited by I. H. Marshall (Elsevier Applied Science, London, 1989) pp. 821–833
10. S. LEE and M. MUNRO, *Composites* **17** (1986) 13.
11. M. J. PINDERA and C. T. HERAKOVICH, *Experimental Mechanics* **26** (1986) 103.
12. M. J. PINDERA, G. CHOKSI, J. S. HIDDE and C. T. HIRAKOVICH, *J. Compos. Mater.* **21** (1987) 1164.
13. C. C. CHAMIS and J. H. SINCLAIR, *Experimental Mechanics* **17** (1977) 339.
14. D. E. WALRATH and D. F. ADAMS, *ibid.* **23** (1983) 105.
15. D. F. ADAMS and D. E. WALRATH, *ibid.* **27** (1987) 113.
16. *Idem*, *J. Compos. Mater.* **21** (1987) 494.
17. D. E. WALRATH and D. F. ADAMS, Verification and application of the Iosipescu shear test method, NASA-CR-174346 (1984).
18. *Idem*, Iosipescu shear properties of graphite fabric/epoxy composite laminates, NASA-CR-176316 (1985).
19. N. K. NAIK and SOM DEV, in Proceedings of the 7th International Congress on Experimental Mechanics held at Las Vegas during June 8–11, 1992, Volume II (The Society for Experimental Mechanics, Inc., Bethel, 1992) pp. 1186–1193.
20. Engineered Materials Handbook, Vol. 1, Composites (ASM International, Metals Park, OH) 1989.
21. J. ABOUDI, *Compos. Sci. Tech.* **33** (1988) 79.
22. N. K. NAIK and V. K. GANESH, in Proceedings of the Second International Symposium on Composite Materials and Structures held at Beijing during August 3–7, 1992 edited by C. T. Sun and T. T. Loo (Peking University Press, Beijing) pp. 938–943.
23. *Idem*, Failure behaviour of plain weave fabric laminates under on-axes uniaxial tensile loading, Report No. IITB/AE/ARDB/STR/659/93/02, IIT, Bombay (1993).
24. *Idem*, Failure behaviour of plain weave fabric laminates under inplane shear loading, Report No. IITB/AE/ARDB/STR/659/93/03, IIT, Bombay (1993).
25. *Idem*, *J. Compos. Tech. and Res.* **16** (1994) 3.
26. J. JORTNER, *Carbon* **30** (1992) 153.

Received 14 April 1994
and accepted 13 February 1996